

AD

TECHNICAL REPORT ARLCB-TR-85029

**ANALYSIS OF ELASTIC-PLASTIC  
BALL INDENTATION TO MEASURE  
STRENGTH OF HIGH STRENGTH STEELS**

AD-A159 882

J. H. UNDERWOOD  
G. P. O'HARA  
J. J. ZALINKA

AUGUST 1985



**US ARMY ARMAMENT RESEARCH AND DEVELOPMENT CENTER  
LARGE CALIBER WEAPON SYSTEMS LABORATORY  
BENET WEAPONS LABORATORY  
WATERVLIET N.Y. 12189**

DTIC FILE COPY

APPROVED FOR PUBLIC RELEASE; DISTRIBUTION UNLIMITED

DTIC  
SEP 10 1985

85 09 12 00M

#### DISCLAIMER

The findings in this report are not to be construed as an official Department of the Army position unless so designated by other authorized documents.

The use of trade name(s) and/or manufacture(s) does not constitute an official indorsement or approval.

#### DISPOSITION

Destroy this report when it is no longer needed. Do not return it to the originator.



20. ABSTRACT (CONT'D)

conditions: using a large ball size and a fixed ratio of indentation depth to ball size; ignoring initial ball contact; accounting for directional material properties; accounting for extraneous system deflections.

Accession for	
NTIS (GSA)	<input checked="" type="checkbox"/>
ERIC	<input type="checkbox"/>
Unannounced	<input type="checkbox"/>
Classification	

5  
 DTIC  
 DTIC  
 DTIC

A1

## TABLE OF CONTENTS

	<u>Page</u>
ACKNOWLEDGEMENTS	111
INTRODUCTION	1
EXPERIMENTS	2
Test Procedures	2
Test Conditions	3
RESULTS AND ANALYSIS	5
Contact Stress and Displacements	5
Finite Element Model	9
Finite Element Results	11
Experimental Results	13
CONCLUSIONS	16
REFERENCES	18

### TABLES

I.    SOME TEST CONDITIONS	4
II.   AVERAGE BALL CONTACT STRESS COMPARED WITH ULTIMATE STRENGTH	6
III.  RELATIONS BETWEEN $d/D$ AND $\delta/D$	7
IV.   COMPARISON OF INDENTATION DISPLACEMENT AND CONTACT STRESS	13

### LIST OF ILLUSTRATIONS

1.    Sketch of indentation test.	19
2.    Plots of indentation load, $P$ , versus change in spacing between ball support and specimen, $\delta_T$ ; $D = 6.35$ mm.	20
3.    Orientations of conventional tension tests and indentation tests.	21

	<u>Page</u>
4. Ideal indentation geometry.	22
5. Ball contact stress versus radial position from finite element model; contact area of diameter, $d$ ; $D = 6.35$ mm; $d/D = 0.25$ ; specimen R1.	23
6a. Comparison of strength calculated from indentation, $\sigma_1$ , to strength measured in tension tests; C orientation; at $\delta = 0.25$ mm; $\sigma_1$ versus $\sigma_u$ .	24
6b. Comparison of strength calculated from indentation, $\sigma_1$ , to strength measured in tension tests; C orientation; at $\delta = 0.25$ mm; $\sigma_1$ versus $\sigma_y$ .	25
7. Comparison of strength calculated from indentation, $\sigma_1$ , to ultimate strength measured in tensile tests; C orientation; at $P = 3.5$ kN.	26
8a. Comparison of strength calculated from indentation, $\sigma_1$ , to ultimate strength measured in tension tests; at $\delta = 0.25$ mm; L orientation indentation versus C orientation tensile.	27
8b. Comparison of strength calculated from indentation, $\sigma_1$ , to ultimate strength measured in tension tests; at $\delta = 0.25$ mm; R orientation indentation versus C orientation tensile.	28

#### ACKNOWLEDGEMENTS

The authors are pleased to acknowledge the help of the following from the Armament R&D Center, R. T. Abbott in conducting experiments, R. F. Haggerty in performing statistical analysis, and R. S. McNeill and E. M. Fogarty in preparing the manuscript. The authors thank D. M. Parks of Massachusetts Institute of Technology for helpful discussions during the analysis of results.

## INTRODUCTION

Ball indentation tests have been used for many years to make estimates of the strength of materials. Perhaps the most familiar use of this sort is the correlation between hardness and ultimate tensile strength (ref 1). One basis for these estimates is the slip-line field analysis of the classic punch problem (ref 2). Although slip-line analysis applies strictly to rigid, perfectly plastic material, it gives a good estimate of indentation contact stresses in many structural materials, particularly those with low rates of strain-hardening. Using results of slip-line analysis and hardness test results, procedures have been developed for estimating the yield strength of steels with strength from about 200 to 600 MPa (ref 3). More recently, Haggag and Lucas (ref 4) described procedures for estimating the key parts of the stress versus strain curve of SAE 1015 steels based on ball indentation tests. Ball indentation tests have also been used as an indirect measure of residual stress (ref 5) by analysis of surface displacements around the indentation.

The central idea of the work here is that if appropriate loads and displacements are measured in physical and numerical experiments of ball

---

<sup>1</sup>Metals Handbook, Taylor Lyman, Ed., The American Society for Metals, 1948, pp. 93-105.

<sup>2</sup>R. Hill, The Mathematical Theory of Plasticity, Oxford University Press, 1950, pp. 254-261.

<sup>3</sup>R. A. George, S. Dinda, A. S. Kasper, "Estimating Yield Strength From Hardness Data," Metal Progress, May 1976, pp. 30-35.

<sup>4</sup>F. M. Haggag and G. E. Lucas, "Determination of Luders Strains and Flow Properties in Steels From Hardness/Microhardness Tests," Metallurgical Transactions A, Vol. 14A, 1983, pp. 1607-1613.

<sup>5</sup>J. H. Underwood, "Residual Stress Measurement Using Surface Displacements Around an Indentation," Experimental Mechanics, Vol. 13, No. 9, 1972, pp. 373-380.

indentation, the interpreted results will give more than an estimate of strength. Within certain ranges of material properties and test conditions, an indentation test can provide an accurate measure of ultimate tensile strength. The objective is to demonstrate that an indentation test of 1000 to 1200 MPa ultimate strength steel can be accurate enough, in some cases, to replace the conventional tension test. The general approach was to perform conventional tests and indentation tests, to model and analyze the indentation tests, and to directly compare the resulting measurements of ultimate strength.

## EXPERIMENTS

### Test Procedures

Figure 1 shows a sketch of the indentation test. A 6.35 mm diameter tungsten carbide ball was pressed into a roughly spherical cavity in the ball support which is attached to the loading head of a universal testing machine. The specimen was a ground surface of the steel being tested. A displacement gage of the type used in fracture toughness testing (ref 6), commonly called a clip gage, was used to measure the displacement  $\delta_T$  between the top of the ball support and the specimen surface.

Load versus indentation displacement plots for two of the conditions tested are shown in Figure 2 to illustrate the general nature of the experimental results. Specimen 185 has the highest strength of the materials

---

<sup>6</sup>"Standard Test Method for Plane-Strain Fracture Toughness of Metallic Materials," E-399-83, 1984 Annual Book of ASTM Standards, Vol. 03.01, pp. 519-554.

tested and specimen R2 has the lowest strength. Note that, although there is noticeable nonlinearity of the plot at low loads, the plot becomes considerably more linear as the load is increased. This may be surprising, since ball indentation is a doubly nonlinear process; that is, the plastic deformation of the specimen is certainly nonlinear, as is the changing contact area feature of ball indentation. It will be shown later that certain aspects of ball indentation geometry combine to produce an approximately linear P versus  $\delta_T$  plot.

In early indentation tests, apparently before the ball was fully seated in the ball support, discontinuities appeared in the P versus  $\delta_T$  plot. These discontinuities were attributed to the ball slipping toward the bottom of the spherical cavity and were not seen again.

The conventional tension tests were performed using the standard ASTM method (ref 7), with a 9.07 mm diameter, shouldered end specimen.

#### Test Conditions

A summary of the material properties, specimens, and orientations included in the investigation is shown in Table I. Conventional tension and indentation tests were performed using pieces from four cylindrical steel forgings. The pieces used for tension test specimens were located immediately adjacent to those for indentation tests. The forgings were made from ASTM A723 steel and varied in overall diameter from about 200 to 300 mm. The yield strength, ultimate strength, and nominal hardness of the pieces of the

---

<sup>7</sup>Standard Methods of Tension Testing of Metallic Materials, E8-83," 1984 Annual Book of ASTM Standards, Vol. 03.01, pp. 130-150.

TABLE I. SOME TEST CONDITIONS

Specimen	Conventional Tensile Tests				Indentation Tests	Hardness		
	Number of Tests	Orientation	Yield Strength $\sigma_{0.1\%}$ , MPa				Ultimate Strength $\sigma_u$ , MPa	
			mean	std. dev.			mean	std. dev.
R1	4	C	1045	14	1149	7	C,R,L	37
R2	4	C	818	55	993	21	C,R,L,	31
R3	4	C	880	8	967	5	C,R,L	31
185	6	C	1220	13	1267	14	C,R,L	41

forgings used for the tests are shown in Table I. The orientation of the tests, shown in upcoming results to be an important variable, is also indicated. The indentation tests were performed in three orientations, circumferential (C), radial (R), and longitudinal (L), as shown in Figure 3. The conventional tension tests were the circumferential orientation.

## RESULTS AND ANALYSIS

### Contact Stress and Displacements

The initial results and preliminary analysis in the investigation were measurement of contact diameters following indentation and, knowing load, calculation of average contact stress; see Table II. Initial indentations were made at a load such that the contact diameter was about 60 percent of the ball diameter,  $d/D = 0.6$ . The average contact stress,  $\bar{\sigma}$ , was calculated from measured load and contact diameter and was compared with the ultimate strengths of the materials. The value of  $\kappa$ , defined as  $\bar{\sigma}/\sigma_u$ , varied from 3.3 to 3.5. Comparison of these values with the value from slip-line field analysis should be revealing. Hill (ref 2) gives the contact stress of a flat punch indentation as:

$$\bar{\sigma} = 2\tau_y(1+\pi/2)$$

where  $\tau_y$  is the shear yield strength. Using the von Mises' yield criterion,  $\sigma_y = \sqrt{3} \tau_y$ , and considering that yield and ultimate strengths are equivalent with regard to slip-line analysis, gives

$$\bar{\sigma} = \kappa\sigma_u = 2.97 \sigma_u \quad (1)$$

---

<sup>2</sup>R. Hill, The Mathematical Theory of Plasticity, Oxford University Press, 1950, pp. 254-261.

The value of  $\kappa$  from Eq. (1), 2.97, is lower than those in Table II, but there are differences in the conditions of these initial experiments and the conditions of the slip-line analysis. Two important differences are that the experimental indenter is not flat and the experimental material has ultimate strengths which are 4 to 21 percent above the yield strengths. Smaller contact diameter relative to ball diameter,  $d/D$ , would minimize the first difference and could help counteract the effects of the second. The testing which followed the initial tests of Table II was performed with smaller values of  $d/D$ .

TABLE II. AVERAGE BALL CONTACT STRESS COMPARED WITH ULTIMATE STRENGTH;  
From Initial Tests;  $D = 6.35$  mm,  $P = 44.5$  kN

Specimen	Contact Diameter $d/D$	Average Contact Stress, $\bar{\sigma}$ MPa	$\frac{\bar{\sigma}}{\sigma_u}$ $\kappa$
R1	0.608	3800	3.31
R2	0.639	3440	3.46
R3	0.647	3550	3.47
185	0.580	4180	3.30

An important requirement which became apparent during initial tests was the need for an indirect measure of contact diameter using a more practicable measurement, such as indentation displacement,  $\delta_T$ . Direct, continuous measurement of  $d$  during indentation would be difficult, and measurements of  $d$  after the indentation can be inaccurate if the specimen surface is not

carefully prepared. An ideal geometric relation between  $d$  and  $\delta$  can be obtained; see Figure 4. Using trigonometry, an exact relation between  $d$  and  $\delta$ , both made nondimensional by  $D$  is

$$\delta/D = \frac{1 - \cos[\sin^{-1} d/D]}{2} \quad (2)$$

An approximate relation, which is simpler to use, is

$$\delta/D = C(d/D)^2 = 0.255(d/D)^2 \quad (3)$$

Table III compares the relations and shows that they are, for most practical purposes, equivalent up to  $d/D$  of about 0.4. Equation (3) gives the reason for the generally linear  $P$  versus  $\delta_T$  plots discussed earlier in relation to Figure 2. Both  $\delta$  and  $P$  vary with  $d^2$ , so they vary linearly with each other.

TABLE III. RELATIONS BETWEEN  $d/D$  AND  $\delta/D$

$d/D$	$\delta/D = \frac{1 - \cos[\sin^{-1} d/D]}{2}$	$\delta/D = C(d/D)^2$ $C = .255$
0	0	0
0.1	0.0025	0.0026
0.2	0.0101	0.0102
0.3	0.0230	0.0230
0.4	0.0417	0.0408

Equations (2) and (3) describe ideal indentation displacements, unaffected by other displacements which can be significant in an actual experiment. The displacement in an actual indentation experiment is always some sort of combined or total displacement,  $\delta_T$ . Figure 1 indicates that the

displacement of the ball support should be considered, so that the total displacement is

$$\delta_T = \delta + \delta_S \quad (4)$$

where  $\delta_S$  is the elastic displacement of the support

$$\delta_S = \frac{[\kappa\sigma_U \pi d^2/4] \ell}{AE} \quad (5)$$

in which  $\ell = 18$  mm, the length of the support, A is the cross-sectional area of the support, and E is elastic modulus. The bracketed term in Eq. (5) is an estimate of load carried by the support, as measured by the indentation variables. Combining Eqs. (3), (4), and (5) gives

$$\delta_T/D = \left\{ 0.255 + \frac{\pi \ell D \kappa \sigma_U}{4AE} \right\} [d/D]^2 \quad (6)$$

an expression which relates  $\delta$  and  $d$ , including both the indentation of the specimen and the displacement of the ball support. The expression should be useful for calculating the amount of extraneous displacement included in a ball indentation test which is performed in the general manner shown in Figure 1. For example, in the case here with  $\ell = 18$  mm,  $D = 6.35$  mm,  $\kappa = 2.97$ , nominal  $\sigma_U = 1200$  MPa,  $A = (19 \text{ mm})^2 \pi/4$ , and  $E = 207,000$  MPa, the quantity  $\delta_T/D$  is  $\delta_T/D = 0.260(d/D)^2$ , about two percent different from Eq. (3).

Another displacement which could conceivably contribute significantly to the total displacement is displacement of the ball. However, the ball is made of tungsten carbide, a high strength and modulus material, and its displacement is expected to be a small fraction of even the two percent effect described by the difference between Eqs. (5) and (6).

### Finite Element Model

Finite element stress analysis was performed in order to identify critical variables in the indentation process, particularly variables which are difficult to evaluate in physical experiments, such as friction effects. The analysis, in general, was an elastic-plastic extension of classic Hertz contact. The details of elastic-plastic ball indentation are quite complex, since they involve an increasing contact area, two-body geometry, and nonlinear elastic-plastic material properties. In this problem the contact area is not known a priori, and the solution method becomes an iterative process to find a result which produces reasonable contact conditions.

The critical location at which proper conditions must be modeled is the point of last contact, point A in Figure 1. At this point, a reasonable solution will be indicated by three tests; (1) the sign of the contact stress will be negative, (2) the stress at point A will be zero, and (3) the deformed surface will be smooth with an inflection point at A. The tests are not independent and the first two are generally used because they can be demonstrated by simple numerical analysis. The best condition to try for in finite element analysis is where the point of last contact, A, is a grid point of the model, and the zero contact stress point appears at A. This is because of the basic assumption of continuous behavior between grid points. If the point of the last contact was between grid points, the contact force would have to be divided between the two grid points and an additional force would have to be applied. This is not an easy condition to simulate.

For this analysis the NASTRAN Rigid Format 6, Piecewise Linear Analysis was used (ref 8), and the rigid ball was analyzed by using an enforced deformation input. This capability is not in the standard version, and an alter package had to be used to produce solutions. Four hundred and fifty elements were used, with fifteen along the radius of contact between ball and specimen. A sixteen piece linear approximation of the stress-strain curve of specimen R1 was used as material properties of the specimen. Stepped constraint was used to simulate a rigid ball, a procedure valid only when the ball modulus is large relative to the base material. The materials used in the experiments have an elastic modulus ratio greater than two. In addition, since this is an elastic-plastic problem, the effective modulus ratio at load is much higher.

Two methods of applying the stepped constraint were attempted in this study. In the first method a constant radius is assumed and the constraint set is expanded to include a greater number of grid points on each step. This requires that two NASTRAN files relating to constraints be generated in a previous step and then read in for each step in the piecewise linear solution. The second method applies a constraint to all grid points on the desired contact surface from the first piecewise linear step, and the correct ball radius is achieved only on the last step. This method assumes that the final result is not path dependent or the path dependence is small.

---

<sup>8</sup>The NASTRAN Theoretical Manual, Level 17.5, NASA SP-221(05), National Aeronautics and Space Administration, December 1980, Section 3.8.

The first method yielded preliminary results that were irregular, and the final contact stress distribution contained unreasonable variations in signs. This was attributed to the fact that each individual step was not a correct solution, and the resulting stresses cannot be extrapolated to the next solution or summed to the correct overall solution. The second method was used to obtain the final results presented here. It yielded smooth contact stress distributions which were easily inspected and plotted to find the correct ball movement. However, three to five computer runs were required to produce the correct solution for each contact radius desired. These two methods could be combined to generate a series of solutions where each solution would expand the size of the contact area by one grid point and use previous solutions as the step to get to that solution. This is a long and expensive process which would require a very large expenditure of computer time.

#### Finite Element Results

Two solutions of ball indentation were obtained. They form the upper and lower bounds of the effect of friction, zero slip with coefficient of friction,  $\mu = \infty$ , and zero friction,  $\mu = 0$ . The distributions of contact stress versus radial position within the contact area are shown in Figure 5. Both distributions are generally constant at about 5000 MPa contact stress and they go to zero at the last contact point,  $r/D = 0.125$ , as required. At the center of the contact area,  $r/D = 0$ , the contact stress becomes positive. This indicates that contact is lost on a small area at the center. However, this area is smaller than the element size and cannot be properly modeled. The distributions also have two odd peaks which may be the result of large

elements.

Values of average contact stress from the two solutions are shown in Figure 5 along with values from an experiment and the slip-line analysis. The experimental value is the measured indentation load divided by the area which is calculated indirectly from measured  $\delta$  using Eq. (3). The value from slip-line analysis was calculated from Eq. (1) using  $\sigma_u = 1149$  for specimen R1, Table I. The higher  $\bar{\sigma}$  value for the zero slip model, compared with zero friction, is believed to be caused by the tangential stress which occurs at the ball-specimen interface when friction is present. The generally higher contact stresses in the model, compared to those from the experiment and slip-line analysis, may be due to too large an element size.

Table IV lists some of the conditions and results from Figure 5 along with others. The higher  $\bar{\sigma}$  values from the model are associated with higher values of indentation displacement,  $\delta$ , as would be expected. Note that the  $\bar{\sigma}$  values from experiment increase with indentation size,  $d$ , and depth,  $\delta$ , and that the three values of  $\bar{\sigma}$  are close to that predicted from slip-line analysis. The best agreement between  $\bar{\sigma}$  from experiment and slip-line analysis was for  $d/D$  of 0.40. The experimental results which follow were obtained with  $d/D$  close to 0.40.

TABLE IV. COMPARISON OF INDENTATION DISPLACEMENT AND CONTACT STRESS

	d/D	δ/D	$\bar{\sigma}/\sigma_u$
<u>Finite Element</u>			
μ = 1.0	0.25	0.021	3.98
μ = ∞	0.25	0.020	3.74
<u>Experiment</u>			
	0.25	0.016	2.80
	0.40	0.042	2.97
	0.108	0.108	3.39
<u>Slip-line Analysis</u>			
	-	0	2.97

Experimental Results

Indentations were made in a ground, flat surface of each of the materials and orientations listed in Table I. Load and displacement were measured, and plots were recorded as indicated in Figures 1 and 2. Upon initial consideration of the results, a method for analyzing the plots was selected which used the slope of the load versus displacement plot as a measure of ultimate strength. The slope method was developed as follows. Using Eq. (1) and the load divided by area definition of  $\sigma$  gives

$$\sigma_u = \frac{4P}{\pi d^2 \kappa}$$

Then, defining  $\sigma_1$  as the ultimate strength of the material determined from indentation and using Eq. (3) gives

$$\sigma_1 = \frac{4CP}{\pi D \kappa \delta}$$

Finally, for a linear P- $\delta$  curve, as generally observed, the result is

$$\sigma_1 = \frac{4C}{\pi D \kappa} \frac{dP}{d\delta} \quad (7)$$

Equation (7) was used to calculate  $\sigma_1$ , a measure of ultimate strength determined from the slope of the P- $\delta$  curve from the indentation test. For the tests and analyses described here, that is, C = 0.255, D = 6.35 mm, and  $\kappa = 2.97$ , the value for a flat indentation in rigid-plastic material, Eq. (7) becomes

$$\sigma_1 = 17.2 \frac{dP}{d\delta}$$

in which  $\sigma_1$  has units of MPa when  $dP/d\delta$  has units of MN/m. Ultimate strength is the product of this constant and the slope of the curve at some appropriate point. Two points on the curve were investigated, a constant displacement,  $\delta = 0.25$  mm, and a constant load, P = 3.5 kN. Note from Figure 2 that these points are generally near the upper end of the P- $\delta$  plot. This avoids any problems which might arise due to the effect of slight irregularities in the ground specimen surface on the measured slope. In the results that follow, slopes were measured manually with no difficulty. Measurement of slopes by computer also could be done.

Figures 6, 7, and 8 are plots of  $\sigma_1$ , ultimate strength determined from indentation tests, versus strength from conventional tension tests. Values of  $\sigma_1$  from each of two indentations are plotted versus the average  $\sigma_u$  or  $\sigma_y$  from that material. A line with slope equal to 1.0 would indicate that  $\sigma_1$  is an

exact measure of  $\sigma_u$  or  $\sigma_y$ .

Figure 6 shows plots of  $\sigma_1$  versus  $\sigma_u$  and  $\sigma_1$  versus  $\sigma_y$ , the 0.1 percent offset yield strength, with all measurements in the C orientation and  $dP/d\delta$  measured at a constant  $\delta = 0.25$  mm. Two linear regression fits of the data are shown, one the standard  $y = mx + b$  form, and the other a nonstandard  $y = mx$  regression. Caution is advised in the use of this second form (ref 9), because the requirement that a line pass through the origin severely limits the general ability of a line to fit data. This form of regression is used here as an indication of how closely  $\sigma_1$  represents  $\sigma_u$  and not as a general best-fit procedure. It is clear from Figure 6 that, as expected (ref 1),  $\sigma_1$  is a better measure of  $\sigma_u$  than it is of  $\sigma_y$ . This is shown by the  $r^2$  correlation coefficient from standard regression and by the  $m$  value from the  $y = mx$  regression.

Figure 7 shows similar results to that of Figure 6a, except that the  $dP/d\delta$  values were taken at a constant load,  $P = 3.5$  kN, rather than at a constant displacement. Neither the  $r^2$  of standard regression nor  $m$  of the  $y = mx$  regression shows a significant difference. Figure 8 gives results in which  $\sigma_1$  for L and R orientations are compared with  $\sigma_u$  from the C orientation. It is clear that mixing orientations results in poor correspondence between  $\sigma_1$  and  $\sigma_u$ .

---

<sup>1</sup>Metals Handbook, Taylor Lyman, Ed., The American Society for Metals, 1948, pp. 93-105.

<sup>9</sup>N. R. Draper and H. Smith, Applied Regression Analysis, Wiley, New York, 1966, pp. 90-91.

It is striking how closely  $\sigma_1$  from ball indentation agrees with conventionally measured ultimate strength. In the results of Figures 6a and 7, in which ultimate strengths in the same orientation were directly compared,  $\sigma_1$  agrees with  $\sigma_u$  within about two percent. Since  $\sigma_1$  was directly calculated from the test conditions and rigid plastic slip-line analysis with no added arbitrary factors, the good agreement indicates that the flat punch approximation of a shallow ball indentation and the rigid-plastic approximation of the steel properties are good approximations. Other factors which contribute to the close agreement are (1) the large ball size relative to surface roughness, and to micro-variations of material properties, (2) the relative insensitivity of the indentation process to friction, as shown by the finite-element model, and (3) the relatively limited range of material properties which was investigated.

#### CONCLUSIONS

The indentation method described here, including the key factors of fixed ratio of indentation depth to ball size, accurate  $dP/d\delta$  measurements, large ball size, and narrow range of material properties, gives an accurate measure of ultimate strength of the high strength steels investigated. The method, when based directly on rigid-plastic analysis, gave results within two percent of the conventionally measured ultimate strength. The indentation method will provide a quick, semi-nondestructive measurement of ultimate strength for a range of high strength steels.

Caution is advised in the use of the method for other materials and with different test conditions. Materials with higher strain-hardening compared

with that of the steels here, will behave much differently. Test conditions basic to the method, such as indentation depth relative to ball size, must be carefully controlled.

## REFERENCES

1. Metals Handbook, Taylor Lyman, Ed., The American Society for Metals, 1948, pp. 93-105.
2. R. Hill, The Mathematical Theory of Plasticity, Oxford University Press, 1950, pp. 254-261.
3. R. A. George, S. Dinda, A. S. Kasper, "Estimating Yield Strength From Hardness Data," Metal Progress, May 1976, pp. 30-35.
4. F. M. Haggag and G. E. Lucas, "Determination of Luders Strains and Flow Properties in Steels From Hardness/Microhardness Tests," Metallurgical Transactions A, Vol. 14A, 1983, pp. 1607-1613.
5. J. H. Underwood, "Residual Stress Measurement Using Surface Displacements Around an Indentation," Experimental Mechanics, Vol. 13, No. 9, 1972, pp. 373-380.
6. "Standard Test Method for Plane-Strain Fracture Toughness of Metallic Materials, E399-83," 1984 Annual Book of ASTM Standards, Vol. 03.01, pp. 519-554.
7. "Standard Methods of Tension Testing of Metallic Materials, E8-83," 1984 Annual Book of ASTM Standards, Vol. 03.01, pp. 130-150.
8. The NASTRAN Theoretical Manual, Level 17.5, NASA SP-221(05), National Aeronautics and Space Administration, December 1980, Section 3.8.
9. N. R. Draper and H. Smith, Applied Regression Analysis, Wiley, New York, 1966, pp. 90-91.

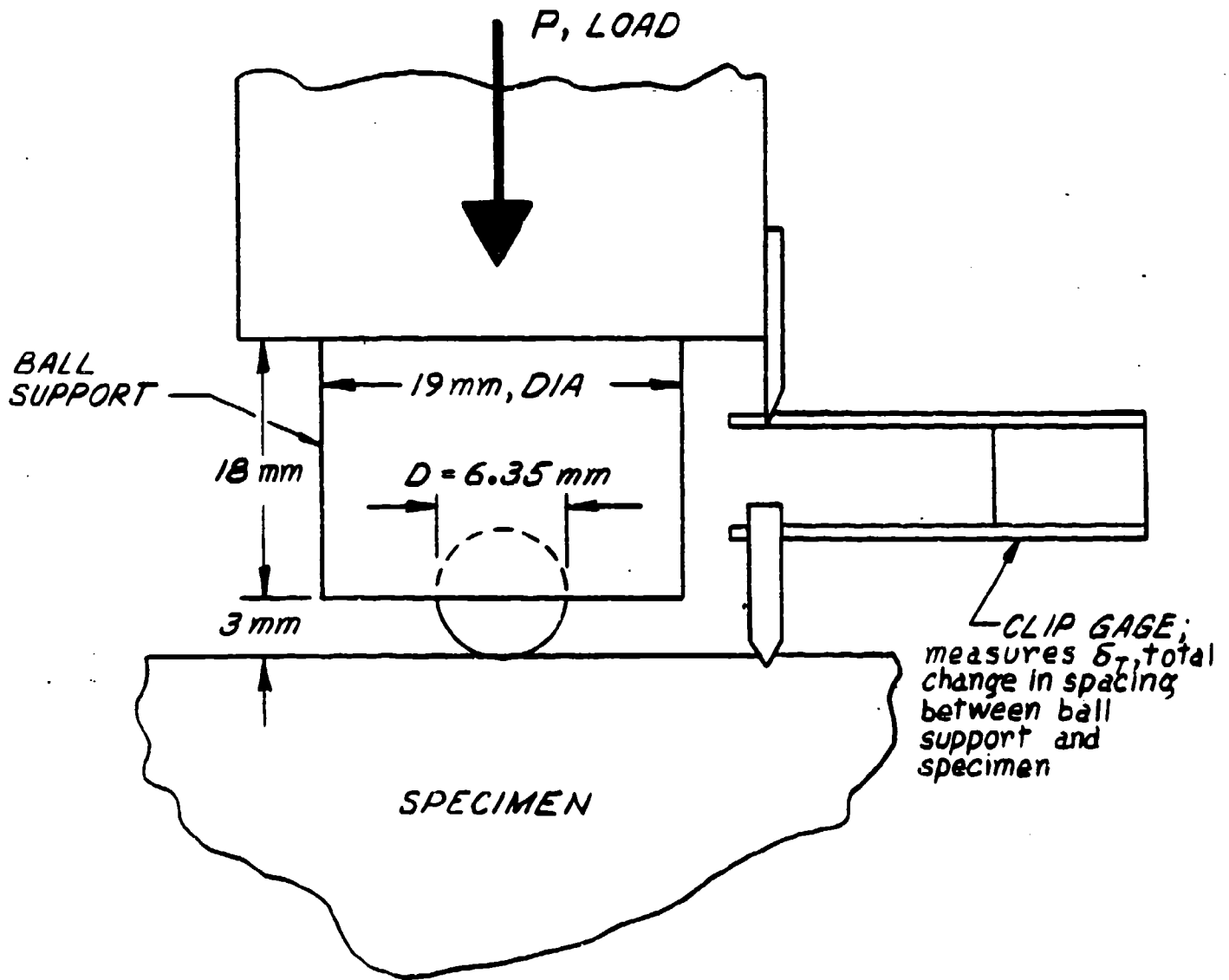


Figure 1. Sketch of indentation test.

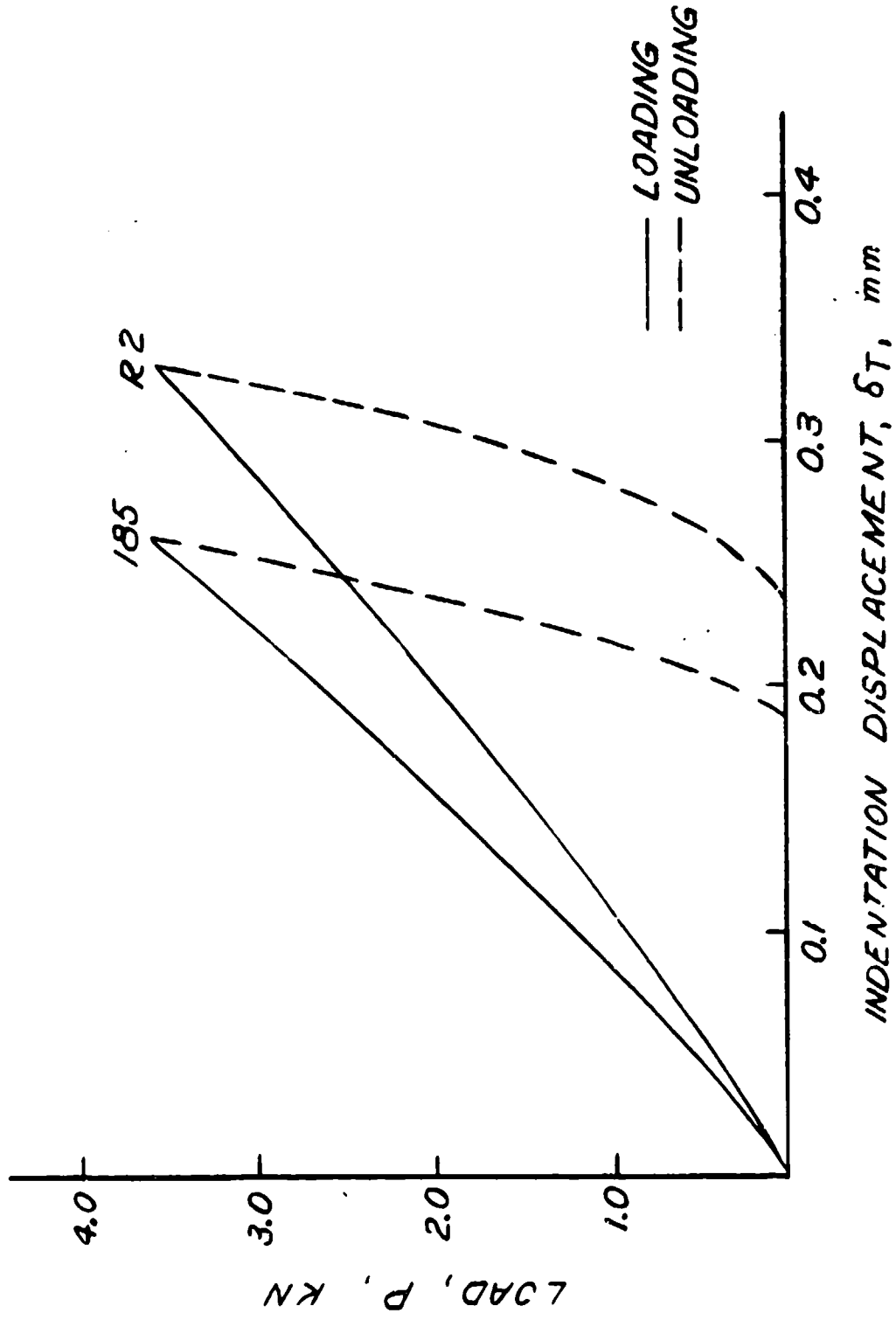


Figure 2. Plots of indentation load, P, versus change in spacing between ball support and specimen,  $\delta_T$ ; D = 6.35 mm.

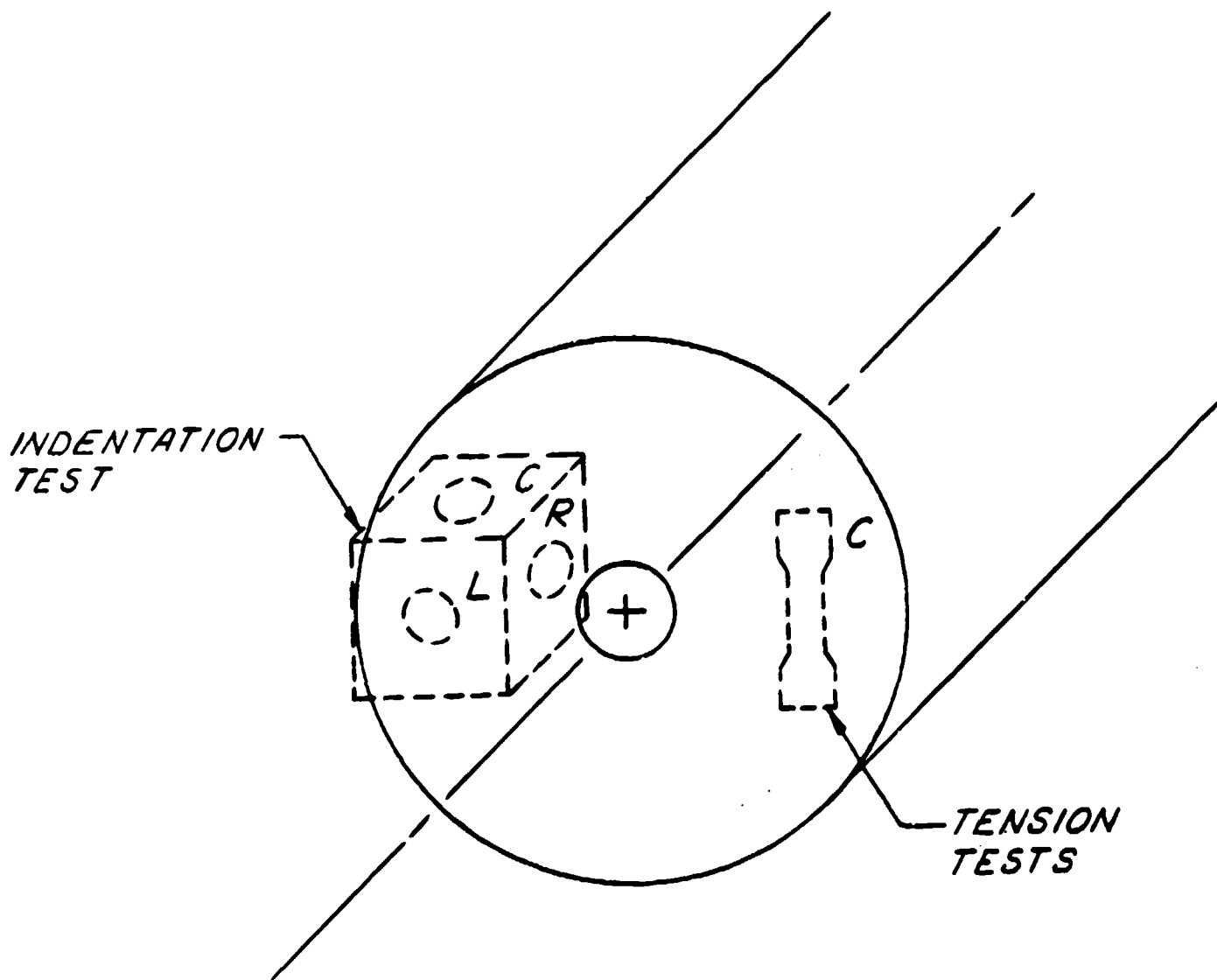


Figure 3. Orientations of conventional tension tests and indentation tests.

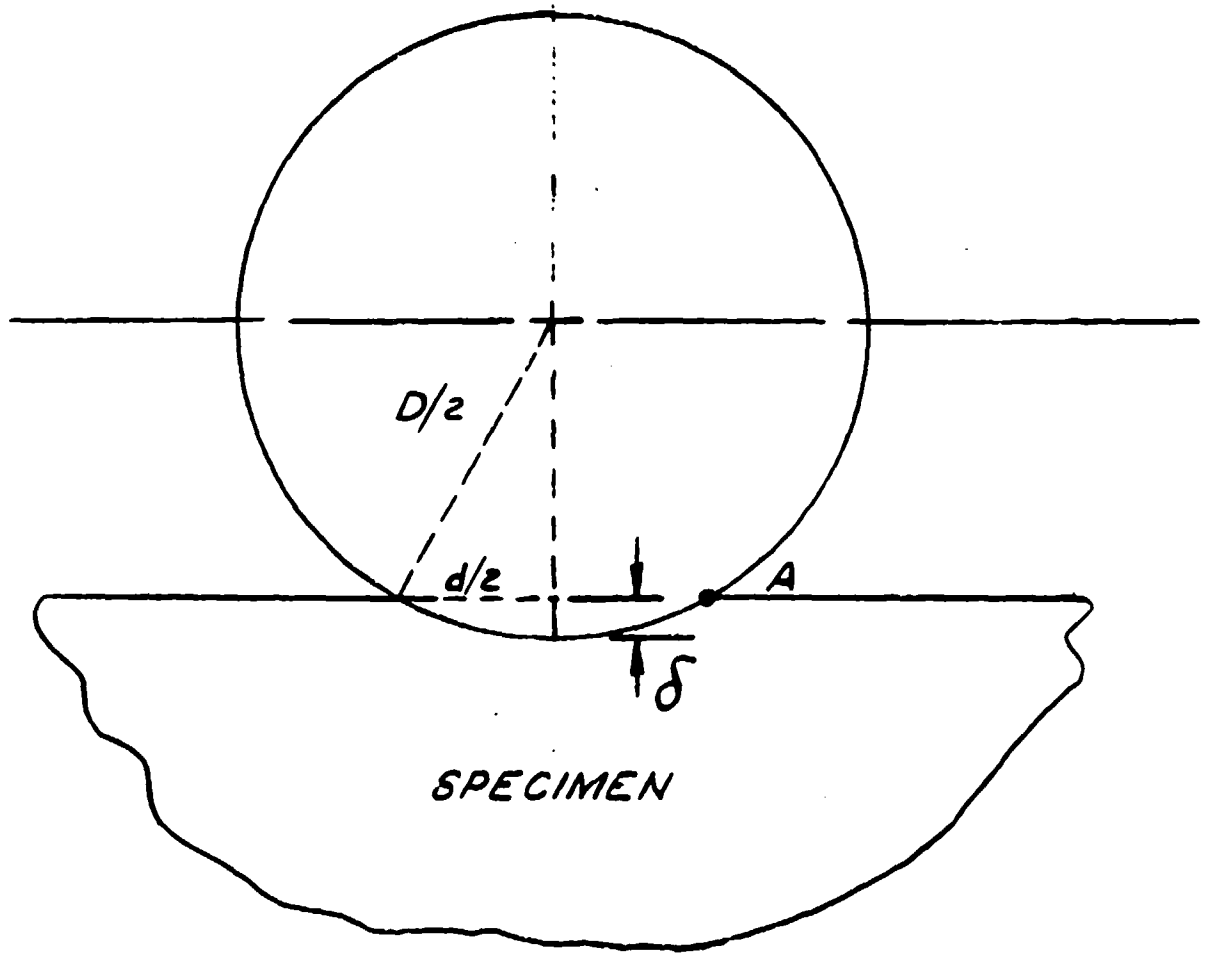


Figure 4. Ideal indentation geometry.

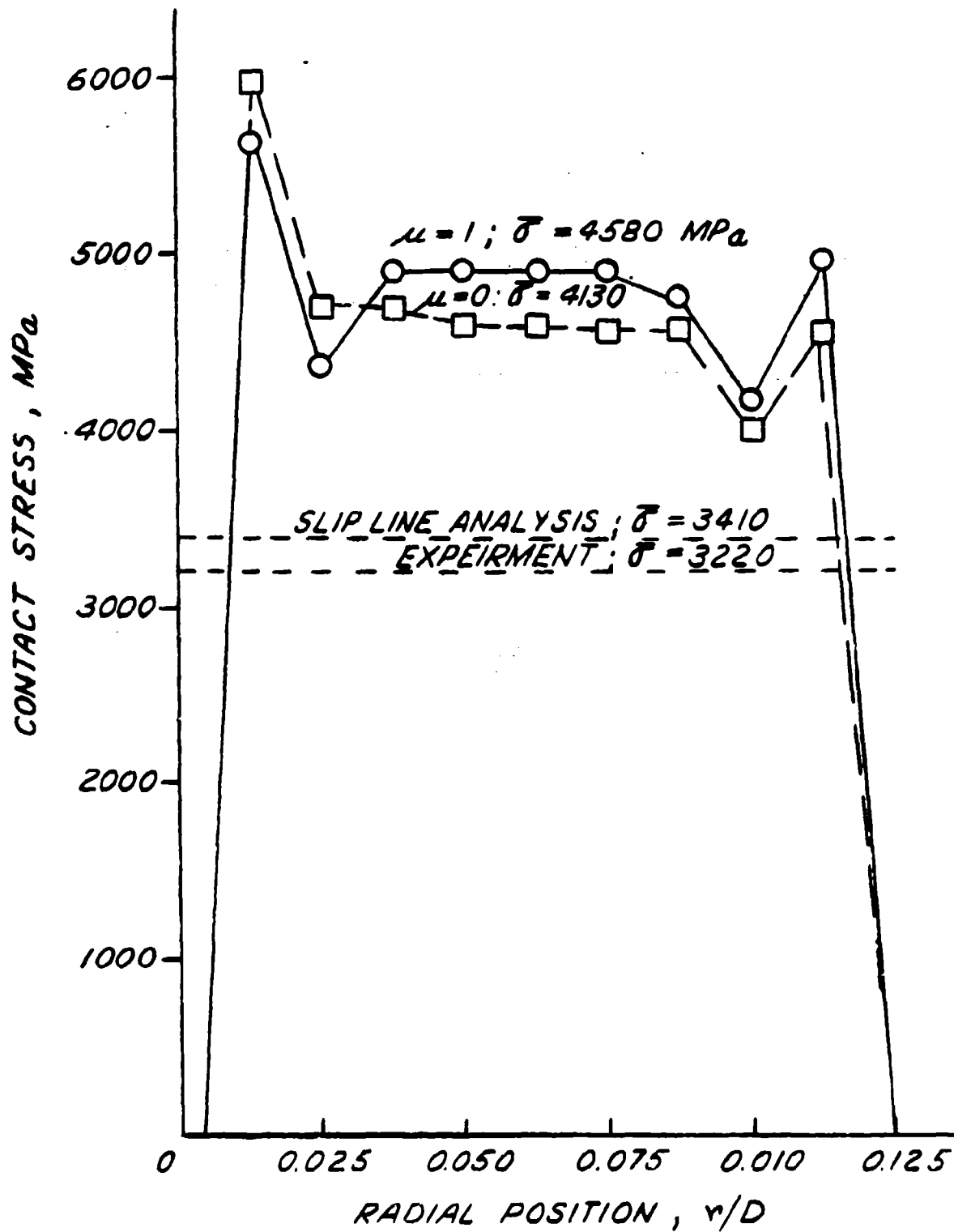


Figure 5. Ball contact stress versus radial position from finite element model; contact area of diameter,  $d$ ;  $D = 6.35 \text{ mm}$ ;  $d/D = 0.25$ ; specimen R1.

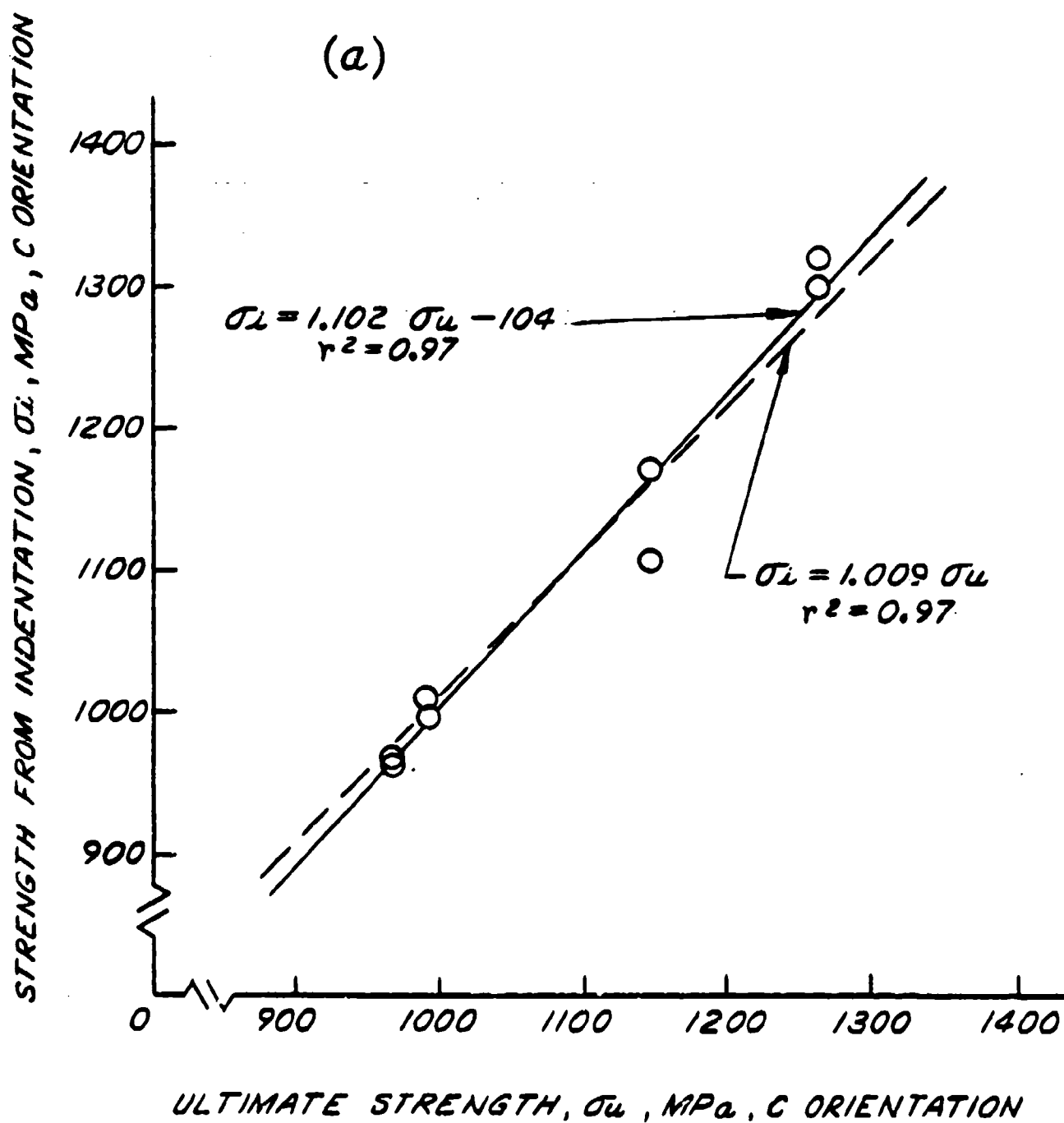


Figure 6a. Comparison of strength calculated from indentation,  $\sigma_i$ , to strength measured in tension tests; C orientation; at  $\delta = 0.25$  mm;  $\sigma_i$  versus  $\sigma_u$ .

STRENGTH FROM INDENTATION,  $\sigma_L$ , MPa, C ORIENTATION

(b)

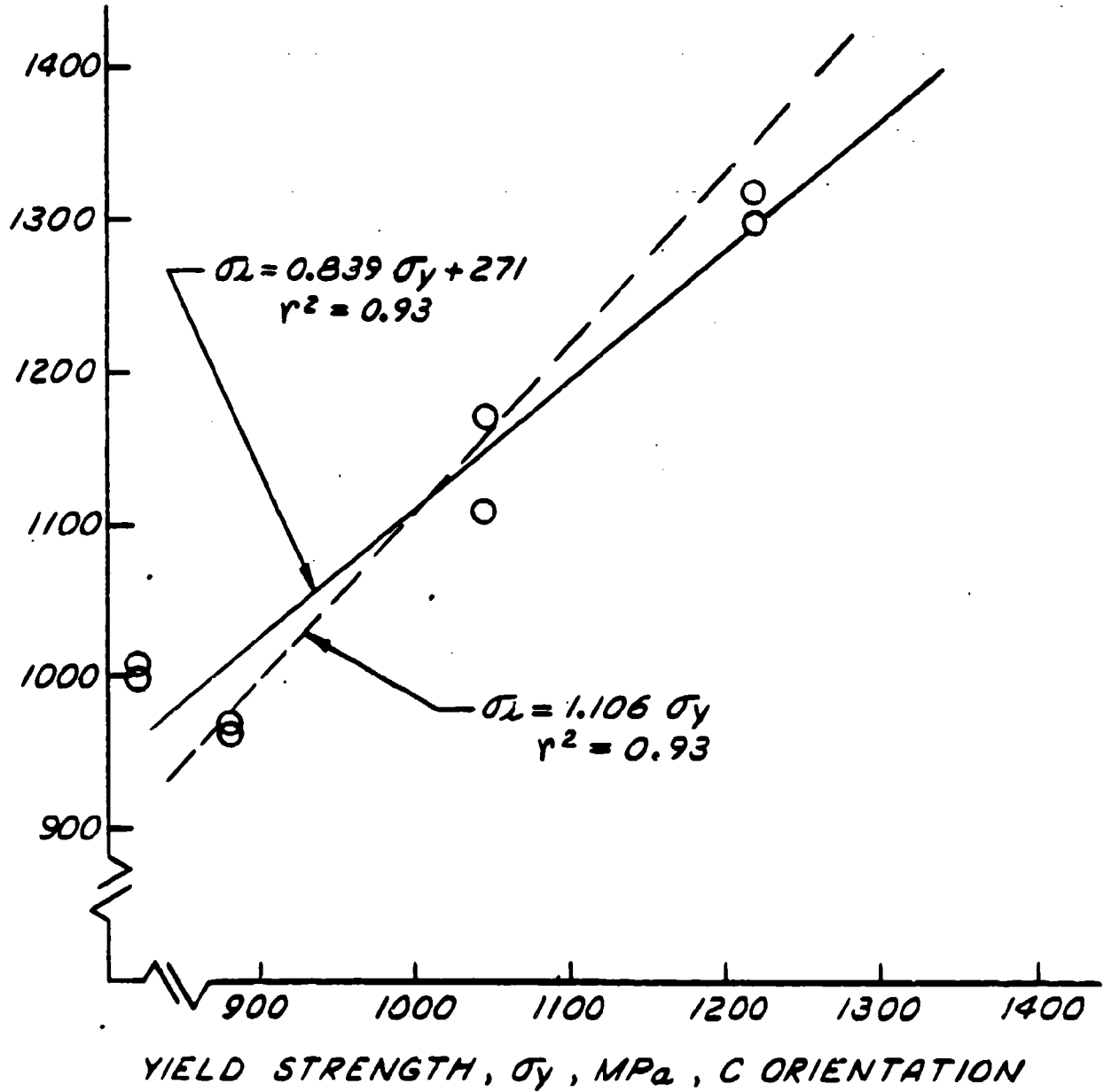


Figure 6b. Comparison of strength calculated from indentation,  $\sigma_i$ , to strength measured in tension tests; C orientation; at  $\delta = 0.25$  mm;  $\sigma_i$  versus  $\sigma_y$ .

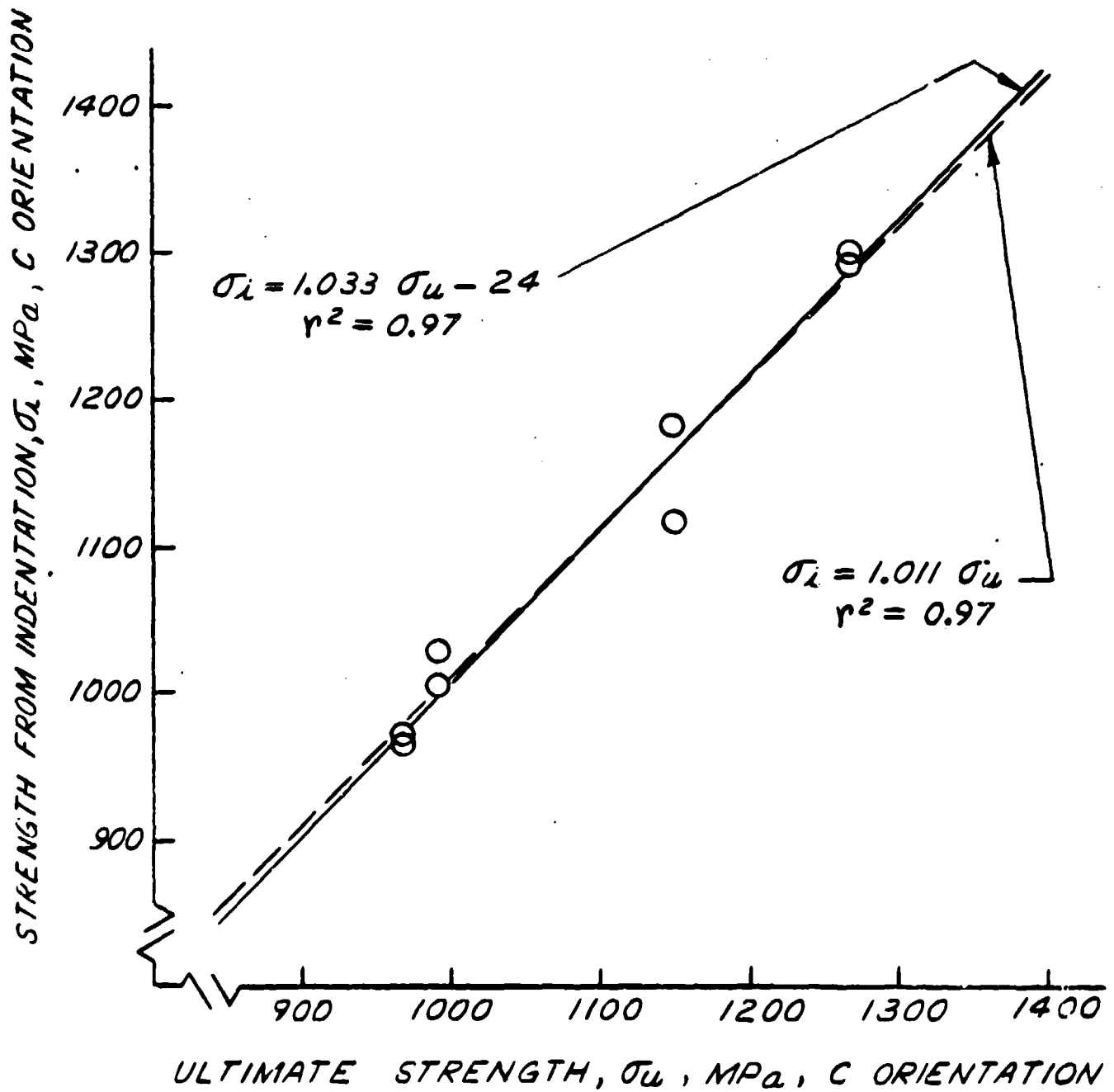


Figure 7. Comparison of strength calculated from indentation,  $\sigma_i$ , to ultimate strength measured in tensile tests; C orientation; at P = 3.5 kN.

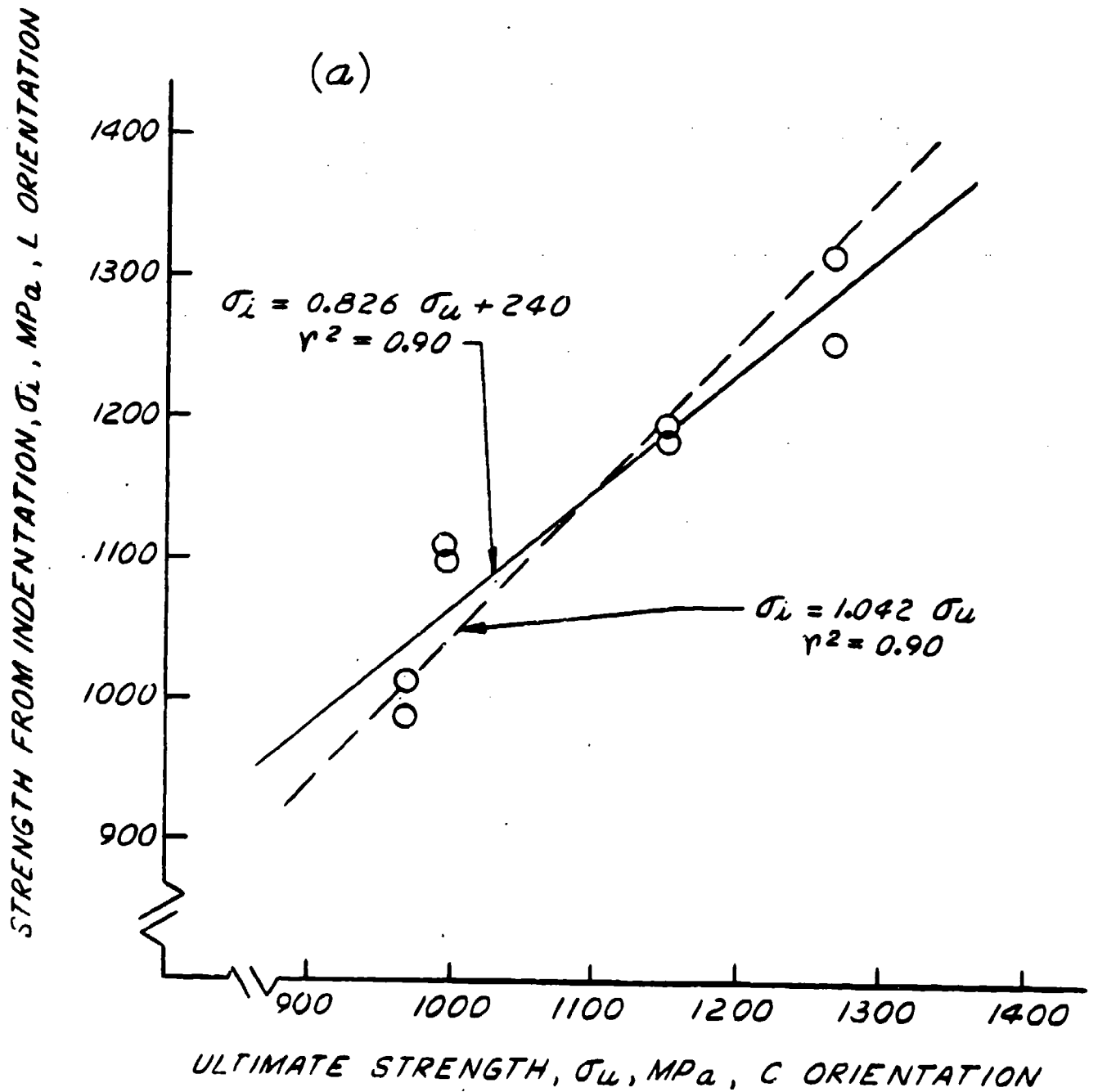


Figure 8a. Comparison of strength calculated from indentation,  $\sigma_i$ , to ultimate strength measured in tension tests; at  $\delta = 0.25$  mm; L orientation indentation versus C orientation tensile.

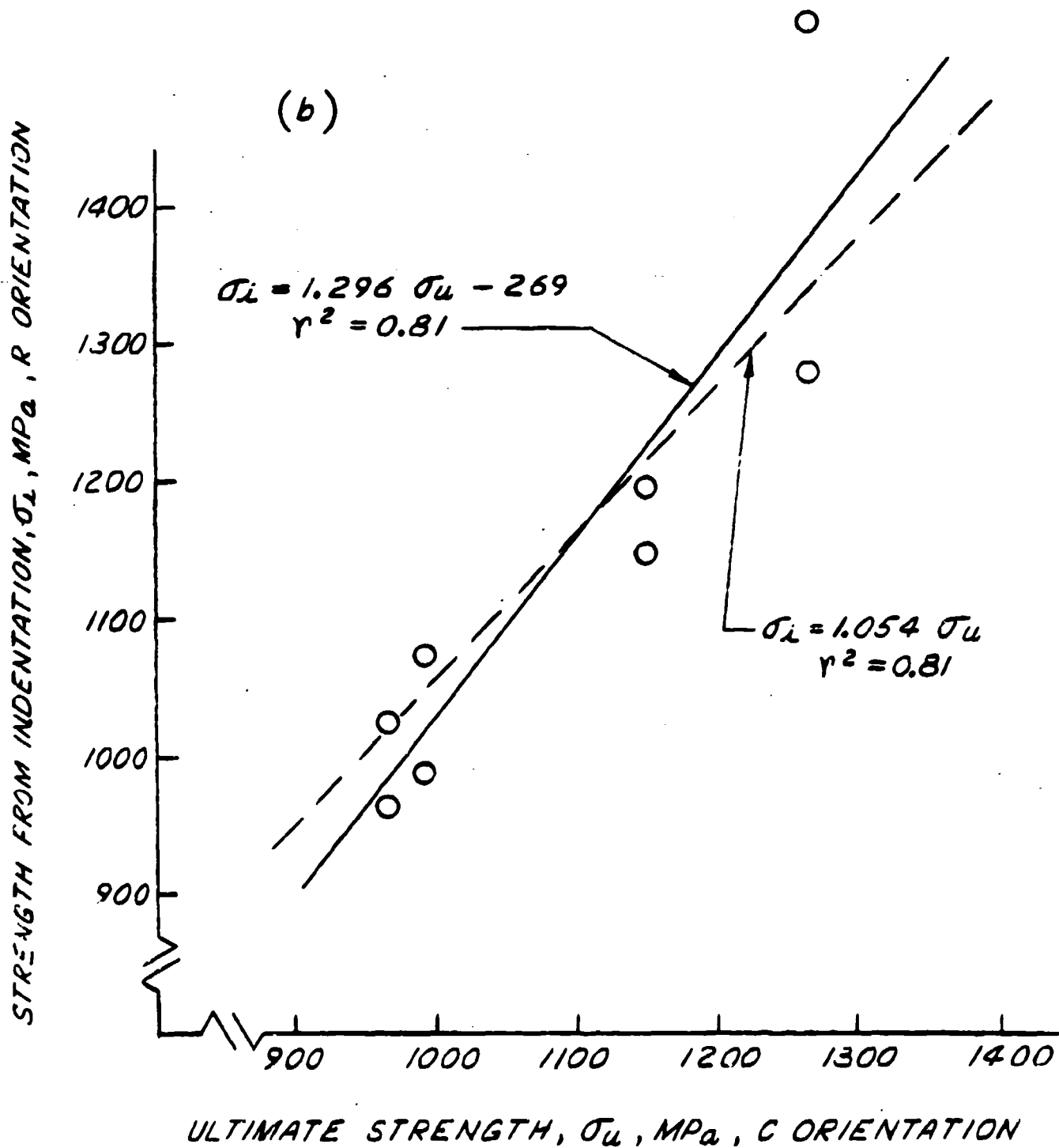


Figure 8b. Comparison of strength calculated from indentation,  $\sigma_i$ , to ultimate strength measured in tension tests; at  $\delta = 0.25$  mm; R orientation indentation versus C orientation tensile.

TECHNICAL REPORT INTERNAL DISTRIBUTION LIST

	<u>NO. OF COPIES</u>
CHIEF, DEVELOPMENT ENGINEERING BRANCH	
ATTN: SMCAR-LCB-D	1
-DA	1
-DP	1
-DR	1
-DS (SYSTEMS)	1
-DS (ICAS GROUP)	1
-DC	1
CHIEF, ENGINEERING SUPPORT BRANCH	
ATTN: SMCAR-LCB-S	1
-SE	1
CHIEF, RESEARCH BRANCH	
ATTN: SMCAR-LCB-R	2
-R (ELLEN FOGARTY)	1
-RA	1
-RM	2
-RP	1
-RT	1
TECHNICAL LIBRARY	5
ATTN: SMCAR-LCB-TL	
TECHNICAL PUBLICATIONS & EDITING UNIT	2
ATTN: SMCAR-LCB-TL	
DIRECTOR, OPERATIONS DIRECTORATE	1
DIRECTOR, PROCUREMENT DIRECTORATE	1
DIRECTOR, PRODUCT ASSURANCE DIRECTORATE	1

NOTE: PLEASE NOTIFY DIRECTOR, BENET WEAPONS LABORATORY, ATTN: SMCAR-LCB-TL,  
OF ANY ADDRESS CHANGES.

TECHNICAL REPORT EXTERNAL DISTRIBUTION LIST

	<u>NO. OF COPIES</u>	<u>NO. OF COPIES</u>
ASST SEC OF THE ARMY RESEARCH & DEVELOPMENT ATTN: DEP FOR SCI & TECH THE PENTAGON WASHINGTON, D.C. 20315	1	COMMANDER US ARMY AMCCOM ATTN: SMCAR-ESP-L ROCK ISLAND, IL 61299 1
COMMANDER DEFENSE TECHNICAL INFO CENTER ATTN: DTIC-DDA CAMERON STATION ALEXANDRIA, VA 22314	12	COMMANDER ROCK ISLAND ARSENAL ATTN: SMCRI-ENM (MAT SCI DIV) ROCK ISLAND, IL 61299 1
COMMANDER US ARMY MAT DEV & READ COMD ATTN: DRUDE-SG 5001 EISENHOWER AVE ALEXANDRIA, VA 22333	1	DIRECTOR US ARMY INDUSTRIAL BASE ENG ACTV ATTN: DRXIB-M ROCK ISLAND, IL 61299 1
COMMANDER ARMAMENT RES & DEV CTR US ARMY AMCCOM ATTN: SMCAR-LC SMCAR-LCE SMCAR-LCM (BLDG 321) SMCAR-LCS SMCAR-LCU SMCAR-LCW SMCAR-SCM-O (PLASTICS TECH EVAL CTR, BLDG. 351N)	1 1 1 1 1 1 1	COMMANDER US ARMY TANK-AUTMV R&D COMD ATTN: TECH LIB - DRSTA-TSL WARREN, MI 48090 1
SMCAR-TSS (STINFO) DOVER, NJ 07801	2	COMMANDER US ARMY TANK-AUTMV COMD ATTN: DRSTA-RC WARREN, MI 48090 1
DIRECTOR BALLISTICS RESEARCH LABORATORY ATTN: AMTR-TSB-S (STINFO) ABERDEEN PROVING GROUND, MD 21005	1	COMMANDER US MILITARY ACADEMY ATTN: CHMN, MECH ENGR DEPT WEST POINT, NY 10996 1
MATERIEL SYSTEMS ANALYSIS ACTV ATTN: DRXSY-MP ABERDEEN PROVING GROUND, MD 21005	1	US ARMY MISSILE COMD REDSTONE SCIENTIFIC INFO CTR ATTN: DOCUMENTS SECT, BLDG. 4484 REDSTONE ARSENAL, AL 35898 2
		COMMANDER US ARMY FGN SCIENCE & TECH CTR ATTN: DRXST-SD 220 7TH STREET, N.E. CHARLOTTESVILLE, VA 22901 1

NOTE: PLEASE NOTIFY COMMANDER, ARMAMENT RESEARCH AND DEVELOPMENT CENTER, US ARMY AMCCOM, ATTN: BENET WEAPONS LABORATORY, SMCAR-LCB-TL, WATERVLIET, NY 12189, OF ANY ADDRESS CHANGES.

TECHNICAL REPORT EXTERNAL DISTRIBUTION LIST (CONT'D)

	<u>NO. OF COPIES</u>		<u>NO. OF COPIES</u>
<b>COMMANDER</b> <b>US ARMY MATERIALS &amp; MECHANICS</b> <b>RESEARCH CENTER</b> <b>ATTN: TECH LIB - DRXMR-PL</b> <b>WATERTOWN, MA 01272</b>	2	<b>DIRECTOR</b> <b>US NAVAL RESEARCH LAB</b> <b>ATTN: DIR, MECH DIV</b> <b>CODE 26-27, (DOC LIB)</b> <b>WASHINGTON, D.C. 20375</b>	1 1
<b>COMMANDER</b> <b>US ARMY RESEARCH OFFICE</b> <b>ATTN: CHIEF, IPO</b> <b>P.O. BOX 12211</b> <b>RESEARCH TRIANGLE PARK, NC 27709</b>	1	<b>COMMANDER</b> <b>AIR FORCE ARMAMENT LABORATORY</b> <b>ATTN: AFATL/DLJ</b> <b>AFATL/DLJG</b> <b>EGLIN AFB, FL 32542</b>	1 1
<b>COMMANDER</b> <b>US ARMY HARRY DIAMOND LAB</b> <b>ATTN: TECH LIB</b> <b>2800 POWDER MILL ROAD</b> <b>ADELPHIA, MD 20783</b>	1	<b>METALS &amp; CERAMICS INFO CTR</b> <b>BATTELLE COLUMBUS LAB</b> <b>505 KING AVENUE</b> <b>COLUMBUS, OH 43201</b>	1
<b>COMMANDER</b> <b>NAVAL SURFACE WEAPONS CTR</b> <b>ATTN: TECHNICAL LIBRARY</b> <b>CODE X212</b> <b>DAHLGREN, VA 22448</b>	1		

**NOTE:** PLEASE NOTIFY COMMANDER, ARMAMENT RESEARCH AND DEVELOPMENT CENTER,  
 US ARMY AMCCOM, ATTN: BENET WEAPONS LABORATORY, SMCAR-LCB-TL,  
 WATERVLIET, NY 12189, OF ANY ADDRESS CHANGES.